REN^{KCTD11} is a suppressor of Hedgehog signaling and is deleted in human medulloblastoma

Lucia Di Marcotullio*†, Elisabetta Ferretti*†, Enrico De Smaele*†, Beatrice Argenti*, Claudia Mincione*, Francesca Zazzeroni‡, Rita Gallo‡, Laura Masuelli*, Maddalena Napolitano*, Marella Maroder*, Andrea Modesti§, Felice Giangaspero*¶, Isabella Screpanti*‖, Edoardo Alesse‡, and Alberto Gulino*¶**

*Department of Experimental Medicine and Pathology and ‖Pasteur Institute, Cenci Bolognetti Foundation, University La Sapienza, 324 Viale Regina Elena, 00161 Rome, Italy; ‡Department of Experimental Medicine, University of L'Aquila, 67100 L'Aquila, Italy; §Department of Experimental Medicine and Biochemical Sciences, University of Tor Vergata, 00133 Rome, Italy; and ¶Neuromed Institute, 86077 Pozzilli, Italy

Edited by Charles J. Sherr, Saint Jude Children's Research Hospital, Memphis, TN, and approved June 7, 2004 (received for review January 30, 2004)

Hedgehog signaling is suggested to be a major oncogenic pathway in medulloblastoma, which arises from aberrant development of cerebellar granule progenitors. Allelic loss of chromosome 17p has also been described as the most frequent genetic defect in this human neoplasia. This observation raises the question of a possible interplay between 17p deletion and the Hedgehog tumorigenic pathway. Here, we identify the human orthologue of mouse REN^{KCTD11}, previously reported to be expressed in differentiating and low proliferating neuroblasts. Human REN^{KCTD11} maps to 17p13.2 and displays allelic deletion as well as significantly reduced expression in medulloblastoma. REN^{KCTD11} inhibits medulloblastoma cell proliferation and colony formation *in vitro* and suppresses xenograft tumor growth *in vivo*. REN^{KCTD11} seems to inhibit medulloblastoma growth by negatively regulating the Hedgehog pathway because it antagonizes the Gli-mediated transactivation of Hedgehog target genes, by affecting Gli1 nuclear transfer, and its growth inhibitory activity is impaired by Gli1 inactivation. Therefore, we identify REN^{KCTD11} as a suppressor of Hedgehog signaling and suggest that its inactivation might lead to a deregulation of the tumor-promoting Hedgehog pathway in medulloblastoma.

brain tumors | tumor suppressor | Gli | 17p deletion

Medulloblastoma (MB), an aggressive neuroectodermal tumor, is the most common childhood brain malignancy, caused by a number of genetic and epigenetic changes affecting the development of cerebellar granule progenitors (1–3).

Allelic deletion on chromosome 17p11.2-pter occurs in up to 50% of MB, with a loss of heterozygosity (LOH) sometimes restricted to a common region at 17p13.2–13.3 (3, 4) that might cause the deletion of one or more genes involved in a tumor suppressor pathway still unidentified.

Deregulation of the Sonic Hedgehog (Shh)-Gli signaling occurs in MB. Shh belongs to the Hedgehog (Hh) family of secreted glycoproteins that trigger the Smoothened (Smo) receptor by relieving the coreceptor Patched (Ptch)-mediated repression. This signal enables downstream Gli transcription factors to regulate expression of target genes involved in the control of developmental processes (i.e., embryonal patterning, cell survival, and growth and tumorigenesis) (5). Germ-line and somatic mutations in components of the Hh pathway [*Ptch*, *Smo* and the Gli-repressor *Su(Fu)*], which lead to activation of ligand-independent signals, have been reported in MB and are suggested to be responsible for tumorigenesis (2, 3, 5). Cerebellar Purkinje cell-secreted Shh promotes the proliferation of granule progenitors (1, 6, 7), indicating that uncontrolled activation of Hh pathway may sustain the development of MB. This hypothesis is confirmed by the development of MB in $Ptc^{-/+}$ mice (8) and by the inhibition of the growth of virtually all MB by cyclopamine, an antagonist of Smo (9, 10). However, mutations of components of Hh pathway occur only in a subset of tumors, indicating additional genetic or epigenetic events that deregulate this pathway. Notably, none of the Hh pathway genes are located in the 17p region frequently deleted in MB.

We have identified REN^{KCTD11} as a murine gene involved in neural progenitor cell proliferation and differentiation (11). *REN* expression is developmentally regulated and restricted to differentiating rather than proliferating neuroblasts of the embryo cortical ventricular zone. Consistently, REN induces growth arrest and differentiation of neural progenitors (11).

Here, we describe the human homologue of murine *REN*, mapping to chromosome 17p13.2. *REN* allelic deletion occurs in 39% sporadic human MB, and its expression is down-regulated in both diploid and, to a higher extent, hemizygous tumors. REN inhibits the growth of MB cells *in vitro* and *in vivo* by antagonizing the Gli-mediated transactivation of Hh target genes. Therefore, we indicate REN as a suppressor of the Shh-Gli pathway, suggesting that its haploinsufficiency in MB might lead to a deregulation of the tumor-promoting Hh signaling, thus representing a potential target for therapeutical intervention.

Methods

Tissue Samples and Cell Cultures. Eighteen specimens of human primary MB (3 desmoplastic and 15 classic histotypes, according to World Health Organization criteria) (12), normal cerebellar, or unaffected peritumoral tissues and 10 glioblastomas were collected during neurosurgery with Institutional Review Board approval, together with blood samples from patients or healthy volunteers, snap frozen in liquid nitrogen, and stored at −80°C. D341, D283, MHHMed3, MEBMed8S, and MHHMed1 cells or Daoy and HEK293 cells were cultured in 20% or 10% heat-inactivated FCS/Hepes/glutamine MEM medium whereas PFSK, SK-N-BE, and SK-N-AS were cultured in 10% FCS/RPMI medium 1640. Cells were transfected with Lipofectamine Plus or Lipofectamine 2000 (Invitrogen). Luciferase activity was assayed with a Dual luciferase assay system (Promega) 24 h after transfection with 0.5 μg of total plasmid DNA per well (including 0.05 μg of luciferase reporter and *Renilla*-expressing vector pRL-TK, Promega).

DNA and RNA Methods. Full-length human *REN* cDNA (accession no. AY646650) was obtained by RACE and PCR cloning (Fig. 6, which is published as supporting information on the PNAS web site). To obtain expression vectors, *REN* was myc-tagged and cloned into pCXN2 (11) or pCDNA3.1 (Invitrogen) or pEGFPN1 (Clontech). ΔPOZ-REN or ΔPOZ$_S$-REN or ΔC-REN mutant expression vectors were constructed by deleting amino acids 18–80 or 51–80 or 196–232, respectively, and inserting into pCDNA3.1.

This paper was submitted directly (Track II) to the PNAS office.

Abbreviations: MB, medulloblastoma; Hh, Hedgehog; Ptch, Patched; Q-PCR, quantitative PCR; Shh, Sonic Hedgehog; Smo, Smoothened.

†L.D.M., E.F., and E.D.S. contributed equally to this work.

**To whom correspondence should be addressed at the * address. E-mail: alberto.gulino@uniroma1.it.

Allelic *REN* dosage and mRNA expression were obtained by real time quantitative PCR (Q-PCR) and RT-Q-PCR respectively (Table 1, which is published as supporting information on the PNAS web site).

Cell Proliferation and Colony Assays. Cell-cycle analysis was carried out on pEGFP or GFP-REN-transfected Daoy cells, fixed after 24 h in 1% paraformaldehyde, stained with 40 μg/ml propidium iodide, and analyzed by flow cytometry in a linear scale by using a FACScan cytometer (Becton Dickinson). BrdUrd incorporation (3- to 24-h pulse) was performed 24 h after transfection (11). For colony assay, 1.4×10^6 Daoy cells were seeded in 10-cm dishes, transfected with pcDNA or pcDNA-RENmyc or pcDNA-ΔPOZ-RENmyc, grown in G418-supplemented medium (600 μg/ml, Sigma) for 2 weeks, and scored for single colonies.

Lentivirus Production and Transduction of Target Cells. Myc-REN was inserted into pWPT vector by replacing GFP, to generate pWPT-REN. Subconfluent 293T cells were cotransfected, by calcium phosphate precipitation, with 20 μg of pWPT-REN or pWPT-GFP, 15 μg of pCMV-DR8.91, and 5 μg of pHCMV-VSVG, to produce REN- and GFP-recombinant lentiviruses (13). After 16 h, medium was changed, and recombinant lentiviruses were harvested 24 h later. Virus titers in supernatants were determined on 293T cells as described (14). D283 cells (1×10^5) were transduced with 1×10^6 recombinant lentivirus-transducing units plus 8 μg/ml Polybrene and 5 days later were harvested and used for xenograft studies.

Xenograft Studies. Six-week-old female athymic BALB/c nu/nu mice (Charles River Breeding Laboratories) were injected s.c. in the flank, with 2×10^6 pWPT-REN or pWPT lentivirus-transduced D283 cells in MEM/Matrigel (Becton Dickinson) (15). After 25 days, the tumors were measured [by using the formula (d1 $\times$ d2 $\times$ d3)/2, for volume evaluation], fixed in 10% formalin, and paraffin-embedded, and 3-μm sections were stained with hematoxylin/eosin or with anti-Gli1 and anti-Ptch1 antibodies (sc6152 and sc6149, Santa Cruz Biotechnology). For ultrastructural analysis, tumors were fixed in 2.5% glutaraldehyde in PBS (pH 7.4) and processed for transmission electron microscopy on a Philips CM10.

Immunostaining and Western Blot Analysis. Western blotting and immunofluorescence were performed as described (11). Antibodies were as follows: anti-GFP (sc-8334) and horseradish peroxidase (HRP)-conjugated anti-mouse IgG (Santa Cruz Biotechnology) and anti-Myc tag [06-549 (Upstate Biotechnology, Lake Placid, NY) and 9E10 (Sigma)]; anti-HA [11MMS-101 P (Babco Covance, Richmond, CA)], Texas red-conjugated anti-rabbit (TI-1000, Vector Laboratories), Alexa Fluor 350-conjugated anti-mouse (A-21049, Molecular Probes).

Results

Allelic Deletion and Decreased Expression of *REN* in Human MB. The human orthologue of murine *REN* has been isolated by RACE (Fig. 6) and mapped, as a single-exon locus, to chromosome 17p13.2 (genomic contig NT010718, synthenic to *REN* bearing mouse chromosome 11) (Fig. 1*A*). REN amino acid sequence is 91% homologue to the murine orthologue (Fig. 7, which is published as supporting information on the PNAS web site).

Human *REN* $\approx$2.9-kb mRNA levels were higher in the cerebellum than in the whole brain and significantly lower in MB cells, the neoplastic counterparts of cerebellar cells (Fig. 1*B*), suggesting that *REN* might be specifically affected in this tumor.

Because 17p13.2 is frequently deleted in MB, we analyzed 18 primary MB and 6 MB cell lines for *REN* ploidy. Q-PCR and loss of heterozygosity of D17S960 microsatellite analysis revealed a deletion of one *REN* allele in 7 of 18 primary tumor samples (39%) and in 4 of 6 MB cell lines examined, compared with diploidy detected in genomic DNA of paired blood cells, in healthy volunteers and in most unrelated brain tumors (glioblastoma) (Fig. 1 *C* and *D* and data not shown).

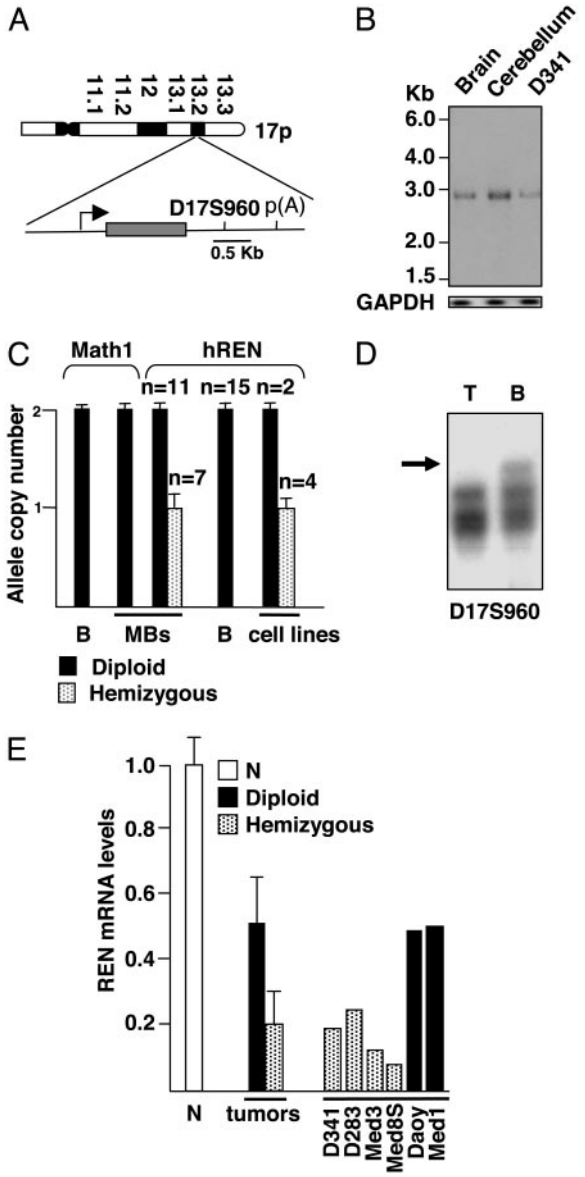

Fig. 1. *REN* is haploinsufficient in medulloblastoma. (*A*) Schematic representation of human *REN* locus. (*B*) Northern blot of *REN* transcripts in human adult whole brain and cerebellum and D341 MB cells. (*C*) Q-PCR of *REN* allele copy number (mean $\pm$ SD) in primary human MB (*n*, number of cases tested; B, blood) and *REN* hemizygous (D341, D283, Med3, and Med8S) and diploid (Daoy and Med1) MB cell lines. The assay for *Math1*, on 4q22, shows the preservation of tumor diploidy. (*D*) Loss of heterozygosity analysis of D17S960 microsatellite in a representative *REN* hemizygous patient (T, tumor specimen; B, paired blood), showing allelic loss (arrow). (*E*) Expression of *REN* mRNA in normal cerebellum (N) [($n = 5$, from normal tissue, peritumoral; Clontech or Ambion (Austin, TX)], primary MB (diploid, $n = 7$; hemizygous, $n = 9$), and MB cell lines was assayed by RT-Q-PCR, normalized with *GAPDH* expression (mean arbitrary units $\pm$ SD). $P < 0.01$ (hemizygous MB vs. normal cerebellum and vs. diploid MB). $P < 0.02$ (diploid MB vs. normal cerebellum) (by Mann–Whitney test).

REN hemizygosity is expected to result in impaired function. Indeed, although the retained allele is unaffected by somatic mutations (as evaluated by DNA sequencing), *REN* transcript levels were 5-fold lower in hemizygous MB cell lines and primary tumors,

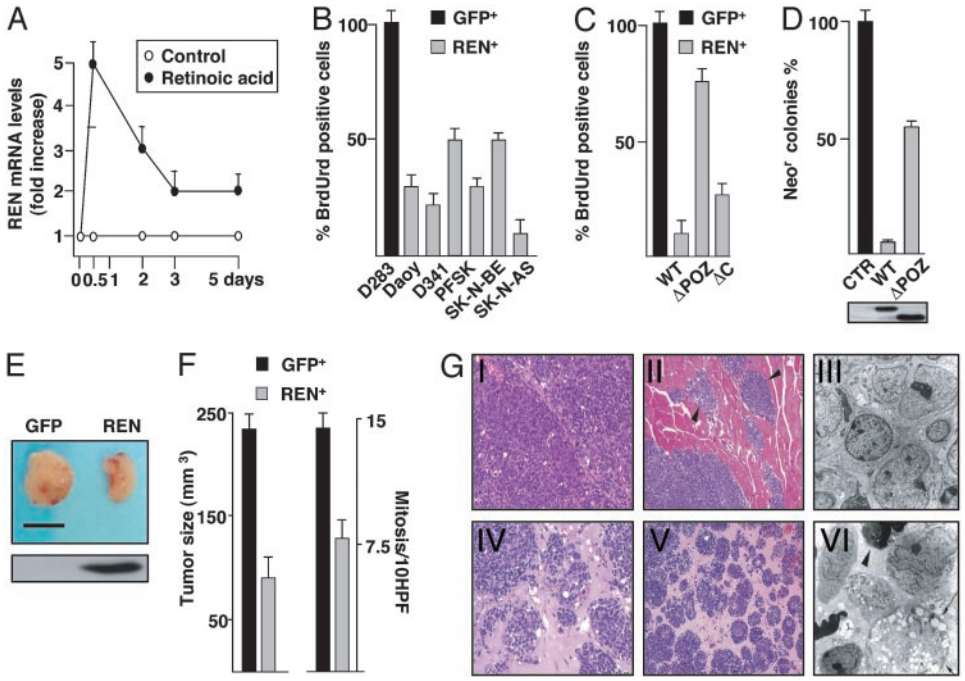

Fig. 2. REN suppresses *in vitro* growth and *in vivo* tumorigenicity of MB cells. (*A*) *All-trans* retinoic acid (1 μM) (Sigma) increases *REN* mRNA levels (assayed by RT-Q-PCR) in D283 cells. (*B* and *C*) BrdUrd-incorporating cells (mean $\pm$ SD from three experiments) 24 h after transfection with pEGFP or Myc-tagged REN (WT) or its deletion mutants (ΔPOZ and ΔC). (*D*) Colony-forming assay of Daoy cells transfected with empty pcDNA (CTR) or myc-tagged REN (WT) or ΔPOZ-REN (ΔPOZ) vectors [average ($\pm$ SD) percentages of colonies, from two triplicate experiments]. (*Lower*) Western blot analysis of cell lysates 24 h after transfection, probed with anti-myc antibody. (*E* and *F*) Representative flank xenografts (bar = 10 mm in *E Upper*), Western blot of myc-tagged REN (stained with anti-myc antibody, *E Lower*), average volumes and mitotic rates ($\pm$ SD) (*F*). Mitotic figures were counted in 20 randomly selected $\times$600 high-powered microscopic fields (HPFs) containing the same number of cells in tumors produced by pWPT-REN and pWPT-GFP lentivirus-transduced D283 cells in athymic nude mice. *, $P < 0.01$ vs. GFP, by Mann–Whitney test. (*G*) Hematoxylin/eosin-stained sections show the reduced cellularity of REN tumor mass with abundant stromal component separating cell clusters (*GIV* and *GV*), compared with the compact cell mass of GFP tumors (*GI*) invading muscle tissue (arrows, *GII*). (Magnification, $\times$20 and $\times$10.) Electron microscopy of REN tumors showing apoptotic (arrowhead) and vacuolated (arrows) cells (*GVI*) compared with GFP xenografts (*GIII*). (Magnification, $\times$2,950.)

compared with normal cerebellar tissue (Fig. 1*E*). Interestingly, $\approx$50% decrease of *REN* mRNA levels was also observed in *REN*$^{+/+}$ primary tumor samples and cell lines (Fig. 1*E*), suggesting that, in addition to allelic loss, MB display a down-regulated *REN* expression occurring by mechanisms that need to be further elucidated.

These results indicate that a haploinsufficient condition due to the loss of 17p13 might be sustained by *REN* transcript levels below a threshold critical for gene function. Haploinsufficiency, due to allelic deletion, has been reported as a likely mechanism for tumorigenesis, when this defect affects genes displaying tumor suppressor functions. Such a mechanism also applies to MB because deletion of a single *Ptc* allele is sufficient to promote the development of cerebellar tumors in *Ptc*$^{-/+}$ mice (16). These observations prompted us to investigate a possible inhibitory role of REN in MB cell growth.

REN Inhibits *in Vitro* Cell Growth and *in Vivo* Tumorigenicity of MB Cells. The expression of murine *REN* is restricted to neuroblasts progressing toward terminal differentiation (11). Accordingly, reti-

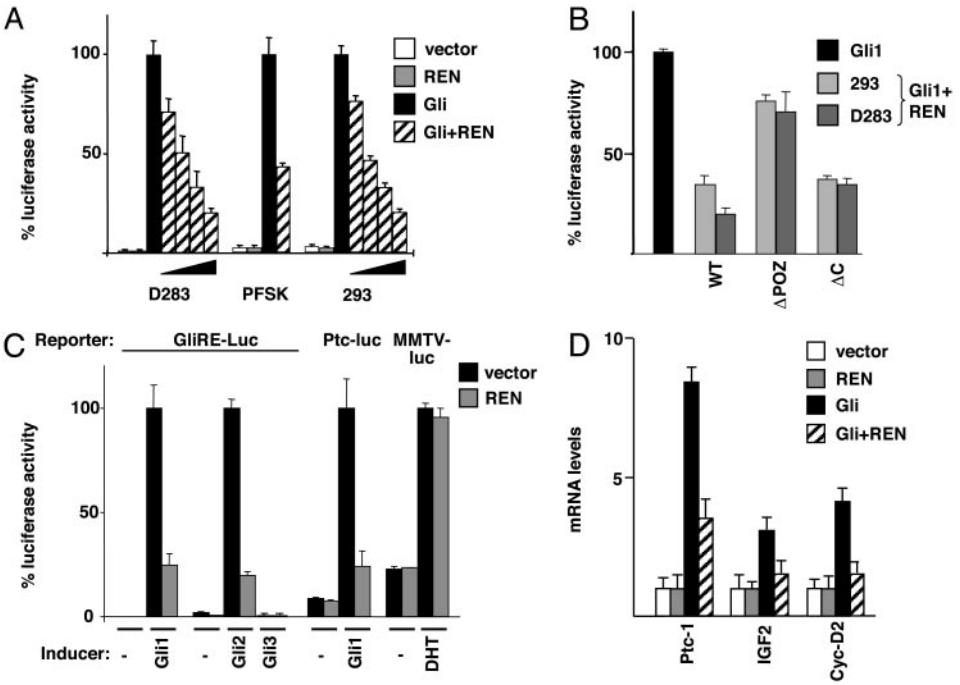

Fig. 3. REN is an antagonist of the Hedgehog pathway. (*A* and *B*) Cells were cotransfected with pCMVHA-Gli1 (32) or WT REN-expressing vectors alone (*A* and *B*) or in combinations (Gli1/REN ratios, 1:0.125 to 1:1) (*A*), or mutant (ΔPOZ, ΔC) (*B*) or empty vectors (*A* and *B*), together with the 3′Gli-BS-luc reporter. Luciferase activity is normalized to the 100% maximum activity driven by the inducer. (*C*) REN inhibits the activation of Gli-RE-luc (containing 12 repeated Gli consensus sequences in a TK minimal promoter vector) and Ptc-luc reporters (19) induced by Gli1 or Gli2 (pCDNAHIS-hGli2) (18) in D283 cells, whereas it does not effect the unrelated MMTV-luc promoter [pGL3-MMTV, containing the MMTV LTR, activated by cotransfected pSG5AR androgen receptor vector and 10^{-7} M dihydrotestosterone (DHT) treatment]. Gli3 vector (18) is inactive on GliRE-luc. (*D*) REN suppresses the Gli1-induced activation of endogenous *Ptch1*, *IGF2*, and *cyclinD2* target genes. RNA from HEK293 cells 24 h after transfection with the indicated plasmids was analyzed by RT-Q-PCR (fold increase with respect to empty vector-transfected cells).

noic acid (RA), which inhibits MB D283 cell growth (15), also enhanced the expression of murine *REN*, which in turn inhibited the proliferation of neural progenitors (11). These observations suggest that REN belongs to a growth inhibitory pathway that might also occur in MB cells. Indeed, the RA-induced growth inhibition of D283 cells correlated with increased expression of *REN* triggered by this drug (Fig. 2*A*).

To investigate whether REN did control the growth of MB cells, we performed BrdUrd labeling of D283, Daoy, and D341 MB cells transfected with either REN or GFP expression vectors. A significant inhibition of BrdUrd incorporation was observed in REN-expressing MB cells and in other human neuroectodermal-derived tumor cell lines (i.e., PFSK, SK-N-BE, and SK-N-AS cells), compared with GFP-transfected controls (Fig. 2*B*). Accordingly, REN inhibited cell-cycle progression, as indicated by a 2-fold reduction in the percentage of Daoy cells in S-G_2/M phase and a corresponding increase of G_1 cells induced by transfection of GFP-tagged REN (S-G_2/M, 13 ± 1%; G_1, 87 ± 2%; $n = 3$) with respect to GFP vectors (S-G_2/M, 25 ± 1%; G_1, 75 ± 2%) (data not shown). Importantly, REN overexpression in D283 or Daoy cells did not increase the percentage of terminal deoxynucleotidyltransferase-mediated dUTP nick end labeling (TUNEL) positive apoptotic cells (data not shown).

Deletion of REN N terminus BTB/POZ domain (ΔPOZ), known to be involved in protein–protein interactions (17), abrogated almost completely its ability to block BrdUrd cell uptake whereas deletion of the C terminus (ΔC) was much less effective (Fig. 2*C*), suggesting that the POZ region is responsible for the growth suppression function.

The colony-forming ability was also significantly suppressed in WT-REN-expressing Daoy cells but not in ΔPOZ-expressing cells (Fig. 2*D*), further suggesting that this domain is critical for REN control of cell proliferation.

Finally, to assess the ability of REN to inhibit MB tumorigenicity, D283 cells were infected with a REN-expressing lentiviral vector and injected s.c. in athymic nude mice. REN-expressing flank xenograft tumors grew to a significantly lower size (38 ± 7% in volume) compared with GFP-expressing tumors analyzed after 25 days (Fig. 2*E*). Histological evidence that REN inhibits tumor growth *in vivo* was a low mitotic rate in REN tumors (Fig. 2*F*) and a reduced tumor mass with scattered cell clusters in an abundant stromal component (Fig. 2 *GIV* and *GV*), compared with GFP-tumors (Fig. 2*GI*), which behaved in a more aggressive way, invading surrounding host tissue (Fig. 2*GII*). Ultrastructural analysis [Fig. 2 *GIII* (GFP) and *GVI* (REN)] showed the presence of large areas of disorganized extracellular matrix, mostly at the periphery of REN tumors. In these areas, vacuolated and dying tumor cells, erythrocytes, fibrinoid degeneration, and hyalinosis were observed, suggesting that REN expression somehow impairs microenvironmental tumor/host tissue interactions.

Together, these findings clearly indicate that REN is able to inhibit the growth of human MB cells *in vitro* and *in vivo*, thus confirming its possible involvement in the antagonism of some specific tumor-promoting pathway.

REN Is an Antagonist of the Hh Pathway. Activation of the Hh pathway has been described as a feature of MB, playing a critical role as a cell growth enhancer and a regulator of cerebellar cell development (1, 6, 7). Therefore, REN tumor suppression property might be due to the ability to down-regulate Hh signaling. To clarify this issue, we first tested the effect of transfected REN on Gli-dependent transcription. Gli1-induced activation of 3′Gli-BS-luc luciferase reporter (driven by a promoter containing Gli-binding sites of the *HNF3β* enhancer) (18), was significantly antagonized by REN (Fig. 3*A*). The POZ domain of REN, responsible for its growth inhibitory activity, is also critical to suppress Gli-dependent gene transcription, as indicated by lack of activity in mutants carrying deletion of either the entire BTB/POZ motif (ΔPOZ) (Fig. 3*B*) or a subdomain (ΔPOZ$_S$; data not shown) whereas ΔC mutant was still effective (Fig. 3*B*). REN also specifically antagonized other Gli-target gene promoters, such as a synthetic promoter consisting of 12 repeated Gli consensus sequence (GliRE-luc) (19) (Fig. 3*C*) or human *Ptch1*, *IGF2*, and *cyclin D2* (5, 20–22), acting on ectopic promoter-driven luciferase reporter (Ptc-luc) and endogenous gene expression (Fig. 3 *C* and *D*). Moreover, the antagonistic ability of REN extended to Gli2, the other downstream transcriptional effector of the Hh pathway (Fig. 3*C*). Conversely, REN cooperated with Gli3 in the abrogation of Gli1 transcriptional activity because Gli3 was devoid of agonistic activity and behaved as a repressor of Gli1-induced transcription (Fig. 3*C* and Fig. 8, which is published as supporting information on the PNAS web site), confirming previous reports (23).

Together these findings strongly support that REN antagonizes Gli1 function.

REN Regulates the Nuclear and Cytoplasmic Localization of Gli1. Gli1 has cytoplasmic or nuclear localization, depending on cell context (19, 23, 24) A major mechanism controlling the activity of Gli1 is represented by the regulation of its cytoplasmic-nuclear shuttling (19, 24). Dyrk1 kinase has been shown to enhance the transcriptional activity by transferring Gli1 into the nucleus (25). To inves-

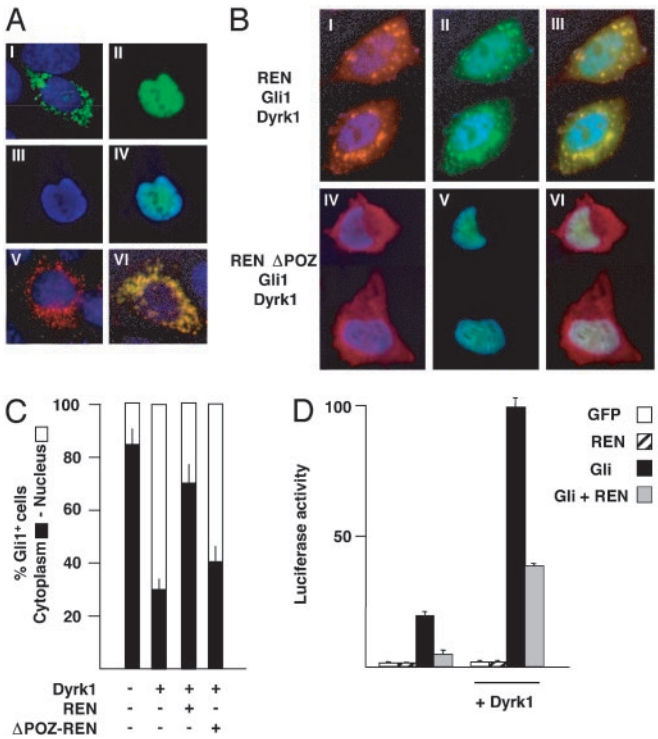

Fig. 4. REN regulates the nuclear and cytoplasmic localization of Gli1. (*A*) Daoy cells were transfected with GFP-tagged Gli1 alone [*AI*; blue indicates 4′,6-diamidino-2-phenylindole (DAPI) nuclear staining] or in combination with hemagglutinin (HA)-tagged Dyrk1 (32) (*AII*, *AIII*, and *AIV*; blue) or REN (*AVI*; red) encoding vectors and analyzed by immunofluorescence microscopy by using mouse anti-HA. Transfection with REN alone is represented in *AV*. (*B*) REN antagonizes Dyrk1-induced Gli1 nuclear transfer. Immunofluorescence staining of Daoy cells cotransfected with GFP-tagged Gli1 (green) and HA-tagged Dyrk1 (blue) in combination with myc-REN or with myc-ΔPOZ-REN (red) encoding vectors. Merging of REN/Dyrk (*BI* and *BIV*), Gli/Dyrk (*BII* and *BV*) and Gli/REN/Dyrk (*BIII* and *BVI*) indicates colocalization of Gli1 and REN (yellow). (*C*) Percentages (mean ± SD of six experiments) of cells showing Gli1 cytoplasmic staining (filled box) or nuclear alone (open box) localization after transfection with the indicated plasmids. At least 150 cells were scored for each coverslip. (*D*) REN antagonizes the transcriptional activity of Gli1 on 3′Gli-BS-luciferase reporter enhanced by cotransfected Dyrk1 in Daoy cells.

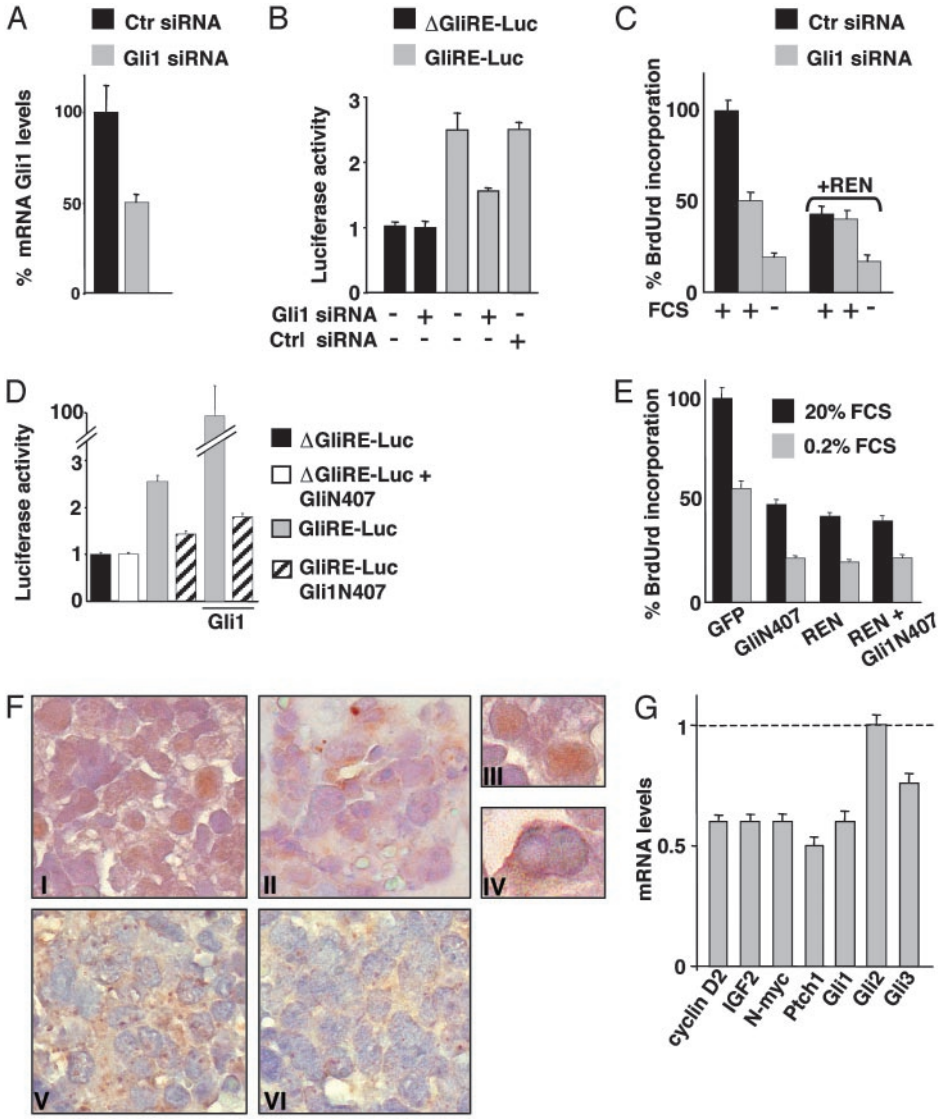

Fig. 5. REN inhibits MB growth by negatively regulating Gli1. (*A*) D283 cells were transfected with either control *siRNA* (no. 1022079, Qiagen, Valencia, CA) or *Gli1 siRNA* (no. 1022368, Qiagen) by using RNAi Fect agent (Qiagen), as suggested by the manufacturer. *siRNA*-transfected cells were assayed for Gli1 mRNA levels by RT-Q-PCR 72 h after transfection. (*B*) Then 0.5 μg of either Gli-RE-luc reporter or the same control reporter vector devoid of Gli consensus sequence (ΔGli-RE-luc) was transfected into D283 cells alone or with control *siRNA* or *Gli1 siRNA*, and luciferase activity was measured after 72 h. (*C*) BrdUrd-incorporating cells (mean ± SD from three experiments) performed 72 h after transfection with control *siRNA* or *Gli1 siRNA* alone or in combination with REN vector in the presence of 20% (+) or 0.2% (−) FCS. (*D*) Gli-RE-luc or ΔGli-RE-luc were transfected into D283 cells along with empty vector or Gli1 or dominant negative Gli1N407 (N407) (mean ± SD from three experiments). (*E*) BrdUrd incorporating cells (mean ± SD from three experiments) 24 h after transfection with GFP, REN, or Gli1N407 as indicated. (*F*) Immunohistochemistry of D283 cell xenografts shows mostly nuclear staining of Gli1 in GFP-infected tumors (*FI* and *FIII*) and a reduced Gli1 staining mostly localized in the cytoplasm in REN-infected tumors (*FII* and *FIV*). A decreased cytoplasmic staining of Ptch1 was also observed in REN-infected (*FVI*) compared with GFP-infected xenografts (*FV*). (*G*) RT-Q-PCR of mRNA expression of the indicated genes in REN tumor xenografts compared with GFP-infected tumors assigned the value 1. Results are expressed in arbitrary units as relative quantification normalized with endogenous control (β-actin and GAPDH).

tigate whether REN may affect the nuclear-cytoplasmic shuttling of Gli1, we determined the subcellular localization of transfected GFP-tagged Gli1, induced to translocate into the nucleus by overexpressed Dyrk1, in the presence or in the absence of coexpressed REN, in Daoy cells. According to previous reports (19, 24), transfected Gli1 is mostly cytoplasmic (Fig. 4*AI*). When coexpressed with Dyrk1, Gli1 fully translocates into the nucleus (ref. 24 and Fig. 4 *AII*, *AIII*, and *AIV*). When REN was cotransfected with Dyrk1, a significant amount of Gli1 was retained in the cytoplasm (Fig. 4 *BI*, *BII*, *BIII*, and *C*). Interestingly, the inactive POZ-domain mutant of REN (Fig. 3*B*) did not modify the nuclear localization of Gli1 induced by Dyrk1 (Fig. 4 *BIV*, *BV*, *BVI*, and *C*).

Although REN is mostly cytoplasmic under basal conditions (Fig. 4*AV*) and colocalizes with cotransfected Gli1 in the cytoplasm (Fig. 4*AVI*), we were unable to coimmunoprecipitate REN and Gli1 (data not shown), suggesting that REN acts upon Gli function by means of an indirect mechanism.

These findings suggest that REN has the property to retain Gli1 in the cytoplasm, under conditions otherwise triggering its nuclear transfer (i.e., Dyrk1 overexpression). According to previous observations (19, 24, 25), the reduced nucleus to cytoplasm ratio of Gli1 induced by REN is consistent with its reduced transcriptional activity. Indeed, Fig. 4*D* shows that Dyrk1 strongly enhanced Gli-luc activity that was instead significantly antagonized by coexpressed REN.

REN Inhibits MB Growth by Negatively Regulating Gli1. Ectopic overexpression of Gli1 induces neural cell hyperplasia (9), including cerebellar granule progenitors (22). Accordingly, exogenous overexpression of Gli1 transcription factor overcomes the inhibition of murine and human MB cell growth induced by cyclopamine, a specific antagonist of the Smo membrane receptor, thus restoring high levels of MB cell proliferation (10).

A role for Gli1 in MB proliferation is specifically indicated by either silencing *Gli1* by *Gli1 siRNA* (Fig. 5 *A–C*) or antagonizing its function by overexpression of a dominant negative Gli1 mutant [N407, deleted of the C terminus (19)] (Fig. 5 *D* and *E*). A reduction of *Gli1* mRNA levels (Fig. 5*A*) and an inhibition of Gli1 transcriptional activity (Fig. 5*B*) by *Gli1 siRNA* results in decreased D283 cell proliferation, as evaluated by BrdUrd incorporation assay (Fig. 5*C*). Similarly, a growth arrest of D283 cells was obtained by inhibition of Gli1 transcriptional function through overexpression of N407 Gli1 mutant (Fig. 5 *D* and *E*).

Because we observed in all MB cell lines investigated a constitutive Gli transcriptional activity, which was inhibitable by REN (Fig. 9, which is published as supporting information on the PNAS

web site), our results suggest that REN led to decreased MB growth by inhibiting Gli1 function. Indeed, we observed that, once the function of endogenous Gli1 is suppressed by *Gli1 siRNA* (Fig. 5 *A* and *B*) or N407 (Fig. 5*D*), REN overexpression does not further inhibit cell growth, the latter being susceptible to be further reduced by serum withdrawal (Fig. 5 *C* and *E*). These findings suggest that Gli1 is required for REN-dependent growth suppressor activity.

Because impaired Gli1 nuclear transfer reduced transcriptional activity (Fig. 4), we decided to verify whether Gli1 inhibition by REN was related to reduced growth of MB *in vivo*, by analyzing the effects of REN on Gli1 subcellular localization in D283 cell xenografts

Fig. 5*F* shows that 74 ± 8% of GFP-infected tumors cells are Gli^+ and most Gli1 immunohistochemical staining is observed in the nucleus (Fig. 5 *FI* and *FIII*). In contrast, REN-infected tumors display 36 ± 5% of Gli^+ cells with a reduced Gli1 staining mostly localized in the cytoplasm (Fig. 5 *FII* and *FIV*).

Reduced Gli transcriptional activity due to Gli1 cytoplasmic relocalization in REN-infected tumor xenografts results in decreased MB tumorigenicity. Indeed, REN-expressing tumors display a reduction of both growth and expression of cell proliferation-related genes, which are direct targets of Gli1 (cyclin D2, IGF2, N-myc) (20, 21, 22) (Fig. 5*G*). A decrease of both Ptch1 (Fig. 5 *FV*, *FVI*, and *G*) and Gli1 (Fig. 5*G*) was also observed in REN-infected xenografts whereas Gli2 or Gli3 expression was unchanged or slightly reduced, respectively (Fig. 5*G*).

Together, these data strongly indicate that REN-induced suppression of Gli activity can inhibit MB growth.

Discussion

Our findings unveil a mechanism of regulation of the Hh pathway by identifying REN as a negative regulator of Gli function. *REN* is haploinsufficient in several human MB, as a consequence of allelic deletion, in association with down-regulated expression. We therefore suggest that the tumor-associated loss of this Hh antagonist may be responsible for the abrogation of a tumor suppression pathway: indeed, REN is provided with a number of tumor inhibitory properties because its overexpression results in inhibition of proliferation *in vitro* and impairment of tumorigenicity *in vivo*. Notably, some of these activities seem to be, at least in part, mediated by its antagonism on Hh signaling because we have shown that REN inhibits the expression of Gli-target genes relevant for cell-cycle progression, such as *cyclin D2*, *N-myc*, and *IGF2*, known to be up-regulated in MB (26, 27). To this regard, IGF2 has been reported to be required for MB tumorigenesis (28). Furthermore, REN growth inhibitory activity is impaired in Gli1 function-deficient MB cells. Therefore, our findings suggest an additional way to hit the Hh pathway in MB, besides the previously described genetic defects targeting individual components of the signaling cascade [i.e., Ptch1, Ptch2, Su(Fu), Smo] (2).

This scenario would allow us to reconsider the role of 17p loss, frequently observed in MB. Allelic loss of *p53*, a putative 17p oncosuppressor in MB, has been reported to cooperate with targeted activation of Hh signaling for murine MB development (29). Therefore, although *REN* and *p53* are not or very rarely mutated in this neoplasia, their hemizygosity-dependent haploinsufficiency might contribute to tumorigenesis, when occurring together with additional defects in distinct pathways. On the other hand, MB-associated activation of Hh signaling occurs more frequently than expected because virtually all human MB tested respond to Hh inhibitors *in vitro* (9, 10) whereas only ≈25% of cases carry mutations in individual components of the pathway (2, 3, 5). Furthermore, murine tumors generated by Hh-unrelated genetic defects (loss of *PARP-1*, *p53*, *DNA Ligase 4*, *Ink4*, and *Kip1*) all result in up-regulation of *Gli*, by still unknown mechanisms (27, 30). Therefore, Hh signaling seems to be primarily affected and does behave as a master oncogenic pathway in experimental MB, as recently highlighted (5, 31). We suggest that haploinsufficiency of the 17p-associated Hh antagonist *REN* might sustain the uncontrolled functional activation of Shh/Gli signaling. These observations might reconcile distinct MB pathogenetic hits in a model in which 17p deletion integrates multiple haploinsufficiency genetic conditions, until they reach a threshold necessary to disclose cooperation with the Hh pathway.

We thank A. Farsetti (Regina Elena Institute, Rome), M. Forni (Regina Mergherita Hospital, Turin, Italy), C. Gambini (Gaslini Hospital, Genoa, Italy), T. Pietsch (University of Bonn, Bonn, Germany), R. Riccardi (Catholic University, Rome), H. Sasaki (RIKEN Center for Developmental Biology, Kobe, Japan), R. Toftgard (Karolinska Institute, Huddinge, Sweden), and D. Wu (University of Connecticut, Farmington) for providing reagents; A. Porcellini, M. Zani, and C. Rinaldi for experimental assistance; and M. Levrero and G. Giannini for critical reading of the manuscript. This work was partially supported by Associazione Italiana per la Ricerca sul Cancro, the National Research Council, the Ministry of University and Research, and the Ministry of Health and Center of Excellence for Biology and Molecular Medicine (BEMM).

1. Wechsler-Reya, R. & Scott, M. P. (2001) *Annu. Rev. Neurosci.* **24,** 385–428.
2. Rubin, J. B. & Rowitch, D. H. (2002) *Cancer Cell* **2,** 7–8.
3. Ellison, D. (2002) *Neuropathol. Appl. Neurobiol.* **28,** 257–282.
4. Steichen-Gersdorf, E., Baumgartner, M., Kreczy, A., Maier, H. & Fink, F.-M. (1997). *Br. J. Cancer* **76,** 1284–1287.
5. Ruiz i Altaba, A., Sanchez, P. & Dahmane, N. (2002) *Nat. Rev. Cancer* **2,** 361–382.
6. Wallace, V. A. (1999) *Curr. Biol.* **9,** 445–448.
7. Dahmane, N. & Ruiz-i-Altaba, A. (1999) *Development (Cambridge, U.K.)* **126,** 3089–3100.
8. Goodrich, L. V., Milenkovic, L., Higgins, K. M. & Scott, M. P. (1997) *Science* **277,** 1109–1113.
9. Dahmane, N., Sanchez, P., Gitton, Y., Palma, V., Sun, T., Beyna, M., Weiner, H. & Ruiz i Altaba, A. (2001) *Development (Cambridge, U.K.)* **128,** 5201–5212.
10. Berman, D. M., Karhadkar, S. S., Hallahan, A. R., Pritchard, J. I., Eberhart, C. G., Watkins, D. N., Chen, J. K., Cooper, M. K., Taipale, J., Olson, J. M., *et al.* (2002) *Science* **297,** 1559–1561.
11. Gallo, R., Zazzeroni, F., Alesse, E., Mincione, C., Borello, U., Buanne, P., D'Eugenio, R., Mackay A. R., Argenti B., Gradini R., *et al.* (2002) *J. Cell Biol.* **158,** 731–740.
12. Giangaspero, F., Bigner, S. H., Kleihues, P., Pitsch, T. & Trojanowski, J. (2000) in *Pathology and Genetics: Tumors of the Nervous System*, eds. Kleihues, P. & Cavenee, W. K. (Int. Agency Res. Cancer, Lyon, France), pp. 129–137.
13. Zufferey, R., Nagy, D., Mandel, R. J., Naldini, L. & Trono, D. (1997) *Nat. Biotechnol.* **15,** 871–875.
14. Bonci, D., Cittadini, A., Latronico, M. V., Borello, U., Aycock, J. K., Drusco, A., Innocenzi, A., Follenzi, A., Lavitrano, M., Monti, M. G., *et al.* (2003) *Gene Ther.* **10,** 630–636.
15. Hallahan, A. R., Pritchard, J. I., Chandraratna, R. A., Ellenbogen, R. G., Geyer, J. R., Overland, R. P., Strand, A. D., Tapscott, S. J. & Olson, J.M. (2003) *Nat. Med.* **9,** 1033–1038.
16. Wetmore, C., Eberhart, D. E. & Curran, T. (2000) *Cancer Res.* **60,** 2239–2246.
17. Bardwell, V. J. & Treisman, R. (1994) *Genes Dev.* **8,** 1664–1677.
18. Sasaki, H., Nishizaki, Y., Hui, C., Nakafuku, M. & Kondoh, H. (1999) *Development (Cambridge, U.K.)* **126,** 3915–3924.
19. Kogerman, P., Grimm, T., Kogerman, L., Krause, D., Unden, A. B., Sandstedt, B., Toftgard, R. & Zaphiropoulos, P. G. (1999) *Nat. Cell Biol.* **1,** 312–319.
20. Yoon, J. W., Kita, Y., Frank, D. J., Majewski, R. R., Konicek, B. A., Nobrega, M. A., Jacob, H., Walterhouse, D. & Iannaccone, P. (2002) *J. Biol. Chem.* **277,** 5548–5555.
21. Louro, I. D., Bailey, E. C., Li, X., South, L. S., McKie-Bell, P. R., Yoder, B. K., Huang, C. C., Johnson, M. R., Hill, A. E., Johnson, R. L., *et al.* (2002) *Cancer Res.* **62,** 5867–5873.
22. Oliver, T. G., Grasfeder, L. L., Carroll, A. L., Kaiser, C., Gillingham, C. L., Lin, S. M., Wickramasinghe, R., Scott, M. P. & Wechsler-Reya, R. J. (2003) *Proc. Natl. Acad. Sci. USA* **100,** 7331–7336.
23. Ruiz i Altaba, A. (1999) *Development (Cambridge, U.K.)* **126,** 3205–3216.
24. Ding, Q., Fukami, S., Meng, X., Nishizaki, Y., Zhang, X., Sasaki, H., Dlugosz, A., Nakafuku, M. & Hui, C. (1999) *Curr. Biol.* **9,** 1119–1122.
25. Mao, J., Maye, P., Kogerman, P., Tejedor, F. J., Toftgard, R., Xie, W., Wu, G. & Wu, D. (2002) *J. Biol. Chem.* **277,** 35156–35161.
26. Pomeroy, S. L., Tamayo, P., Gaasenbeek, M., Sturla, L. M., Angelo, M., McLaughlin, M. E., Kim, J. Y., Goumnerova, L. C., Black, P. M., Lau, C., *et al.* (2002) *Nature* **415,** 436–442.
27. Lee, Y., Miller, H. L., Jensen, P., Hernan, R., Connelly, M., Wetmore, C., Zindy, F., Roussel, M. F., Curran, T., Gilbertson, R. J. & McKinnon, P. J. (2003) *Cancer Res.* **63,** 5428–5437.
28. Hahn, H., Wojnowski, L., Specht, K., Kappler, R., Calzada-Wack, J., Potter, D., Zimmer, A., Muller, U., Samson, E., Quintanilla-Martinez, L., *et al.* (2000) *J. Biol. Chem.* **275,** 28341–28344.
29. Wetmore, C., Eberhart, D. E. & Curran, T. (2001) *Cancer Res.* **61,** 513–516.
30. Tong, W. M., Ohgaki, H., Huang, H., Granier, C., Kleihues, P. & Wang, Z. Q. (2003) *Am. J. Pathol.* **162,** 343–352.
31. Ruiz i Altaba, A., Stecca, B. & Sanchez, P. (2004) *Cancer Lett.* **204,** 145–157.
32. Dunaeva, M., Michelson, P., Kogerman, P. & Toftgard, R. (2003) *J. Biol. Chem.* **278,** 5116–5122.